Journal of Earth Science, Vol. 21, No. 6, p. 941–953, December 2010 ISSN 1674-487X
Printed in China
DOI: 10.1007/s12583-010-0147-4

Assessment of Soil Erosion and Sediment Yield in Liao Watershed, Jiangxi Province, China, Using USLE, GIS, and RS

Li Hui* (李辉)
Faulty of Earth Sciences, *China University of Geosciences*, *Wuhan* 430074, *China*; *Three Gorges Research Center for Geo-hazard*, *Ministry of Education*, *China University of Geosciences*, *Wuhan* 430074, *China*
Chen Xiaoling (陈晓玲)
The Key Lab of Poyang Lake Ecological Environment and Resource Development, *Jiangxi Normal University*, *Nanchang* 330022, *China*; *State Key Laboratory for Information Engineering in Surveying*, *Mapping and Remote Sensing*, *Wuhan University*, *Wuhan* 430072, *China*
Kyoung Jae Lim
Department of Agricultural Engineering, *Kangwon National University*, *Chuncheon*, *Kangwon*, *200-701*, *Korea*
Cai Xiaobin (蔡晓斌)
Institute of Geodesy and Geophysics, *Chinese Academy of Sciences*, *Wuhan* 430077, *China*
Myung Sagong
Track & Civil Engineering Research Department, *Korea Railroad Research Institute*, *Uiwang*, *Kyunggi-do*, 437-050, *Korea*

ABSTRACT: Soil erosion by water is a serious problem all over the world. In China, about 1 790 000 km^2 of land suffers from water erosion, which accounts for 18.3% of China's total area. This study was conducted in the Liao (潦) watershed in Jiangxi (江西) Province to assess annual soil erosion and sediment yield using the Universal Soil Loss Equation (USLE). A geographic information system (GIS) was used to generate maps of the USLE factors, which include rainfall erosivity (*R*), soil erodibility (*K*), slope length and steepness (*LS*), cover (*C*), and conservation practice (*P*) factors. By integrating these factors in a GIS, a spatial distribution of soil erosion over the Liao watershed was obtained. The soil erosion was found to vary from nil for flat and well-covered areas to more than 500 t/ha/a in mountainous places with sparse vegetation. The average soil erosion is 18.2 t/ha/a with a standard deviation of 109.3 t/ha/a. The spatial distribution of erosion classes was estimated. About 39.5% of the watershed is under the tolerant erosion rate, and 60.5% of the study area experienced erosion to different extents. A spatially distributed sediment delivery ratio (SDR) module was developed to account for soil

This study was supported by China Technological Supporting Program (No. 2007BAC23B05), the Special Research Fund for Prevention of Geological Disasters in Three Gorges Reservoir Area (No. SXKY3-6-1), the Natural Science Foundation of Hubei Province (No. 2009CDB104), and the Opening Foundation of State Key Laboratory for Information Engineering in Surveying, Mapping, and Remote Sensing, Wuhan University (No. (09)Key 01).
*Corresponding author: leelmars@gmail.com

Manuscript received July 13, 2010.
Manuscript accepted September 10, 2010.

erosion and deposition. It was found that the SDR value at the outlet of the Liao watershed was 0.206, and the sediment yield was 1.32 million t/a, which was 20% higher than the measured sediment. The results can be used to identify the soil erosion hot spots and develop the best soil erosion management practices and help estimate the quantity of soil that was transported into the downstream Poyang (鄱阳) Lake.

KEY WORDS: soil erosion, USLE, GIS, sediment delivery ratio.

INTRODUCTION

Accelerated soil erosion has been globally recognized as a serious problem since people took up agriculture (Renschler et al., 1999). Soil erosion affects soil productivity by changing soil properties and particularly by destroying topsoil structure, reducing soil volume and water holding capacity, reducing infiltration, increasing run-off, and washing away plant nutrients, such as nitrogen, phosphorous, and organic matter (Oyedele, 1996; Meyer et al., 1985). The resulting soil particles themselves act as the carrier of pollutants including heavy metals, nutrients, pesticides, and other materials and increased levels of sedimentation in lakes, damaging water quality and leading to eutrophication (Bakoariniaina et al., 2006; Flügel et al., 2003).

The watershed prioritization and formulation of proper watershed management programs for sustainable development require information on soil erosion and sediment yield (Pandey et al., 2007). However, it is difficult to model soil erosion because of the complexity of the interactions of factors that influence the erosion process (Wischmeier and Smith, 1978). Substantial efforts have been invested in developing soil erosion models resulting in a variety of models that range from simple empirically orientated equations, such as the Universal Soil Loss Equation (USLE) (Wischmeier and Smith, 1978) and its revised version, RUSLE (Renard et al., 1997), to more sophisticated models, such as the Water Erosion Prediction Project (WEPP) (Nearing et al., 1994) and EUROSEM (Morgan et al., 1998). The latter may be functionally more powerful than the empirical models, but those models often need lots of data and are computationally intensive to use in many circumstances, particularly with respect to modeling soil erosion in medium- and large-scale watersheds (Wang et al., 2009). On the contrary, the USLE has been extensively applied all over the world at many scales mainly due to the simplicity of the model formulation and easy availability of the dataset (Wang et al, 2009; Pan et al., 2005; Shi et al., 2004; Bartsch et al., 2002; Jain et al., 2001; Jain and Kothyari, 2000). An effective investigation of soil erosion within a watershed by USLE requires spatially distributed data of several parameters describing the watershed. The latest advances in remote sensing (RS) techniques provide spatial information that is normally difficult to obtain, especially in the developing countries (Bakoariniaina et al., 2006; Fistikoglu and Harmancioglu, 2002). GIS tools can facilitate derivation of the topographic factor from DEM's data and computation of soil losses (Wang et al., 2003; Bartsch et al., 2002; Cerri et al., 2001). GIS is also capable of quantification of heterogeneity of a watershed by discretizing it into subareas, each having approximately homogeneous characteristics (Rodda et al., 1999; Young et al., 1987). Thus, the integration of RS and GIS technologies with USLE has proven to be an efficient tool and has been successfully used by various investigators for soil erosion assessment (Bahadur, 2009; Ozcan et al., 2008; Bhattarai and Dutta, 2007; Shi et al., 2004).

The USLE estimates gross sheet and rill erosion but does not calculate sediment delivered to the downstream point of interest. As a result, the sediment delivery ratio (SDR) was introduced. Fistikoglu and Harmancioglu (2002) used empirical relationships between the SDR and the watershed area in order to compute sediment load to the Gediz River, Turkey. The WinGrid system by Lin et al. (2002) considered the SDR based on receiving drainage length ratio to total drainage length to compute soil erosion and sediment yield using USLE and a sediment delivery ratio. Lim et al. (2005) fully integrated an area-based SDR module with a GIS system and developed the Sediment Assessment Tool for Effective Erosion Control (SATEEC). Zhou and Wu (2008) divided a 15 378 km^2 watershed into six hydrological units (HU) and computed the SDR for each of them based on transported sediment to HU outlets and mean soil loss in the HU when assessing soil erosion and sediment delivery ratio with USLE. Beskow et al. (2009) estimated SDR using a similar method as Zhou and Wu (2008) in order to validate the soil erosion simulation process in the Grande River basin. It is obvious that most of the works mentioned above are based on the lumped concept; however, few take into account the spatial variation. The lumped method worked well for comparatively uniform units but did not work as well in topographically complex areas. Therefore, this article presents further improvements of the previous works by reconsidering the methodology of SDR in a distributed manner.

The objectives of this article are (1) to estimate soil erosion for the Liao watershed, China, using USLE, RS, and GIS with publicly available information and (2) to determine the amount of sediment transported to the downstream Poyang Lake using the proposed spatially distributed SDR module.

STUDY AREA

The Liao watershed with an area of 3 530 km^2 is part of the larger Poyang Lake drainage basin of 162 200 km^2. The lake is located in Jiangxi Province and is the largest fresh water lake in China and is an important international wetland with considerable ecosystem functions (Fig. 1). The Liao River is one of the major rivers that drain into the Poyang Lake. The Liao watershed is characterized by very steep slopes on the hillsides and gentle slopes in its middle and lower reaches where the surface is extensively cultivated. The elevation varies from 13 to 1 772 m asl with a mean value of 342 m asl. The slope ranges from 0° to 52° with a mean value of 4.03°. The watershed is situated in a subtropical zone with a monsoonal climate. The mean annual precipitation is 1 613.7 mm, of which 73.1% occurs from March to August. The mean annual temperature is 16.5 ℃, and the hottest months, July and August, reach almost an average temperature of 28 ℃. The major soil types include red soil, weakly developed red soil and brown soil. The land use types mainly include forest, agriculture, grassland, shrub, water body, urbanization and traffic, and bare soil (Fig. 2).

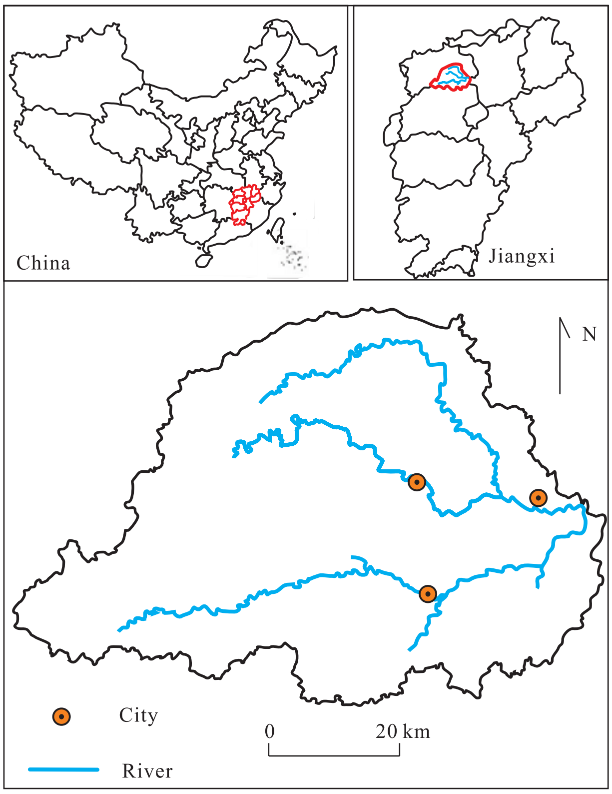

Figure 1. Location of Liao watershed.

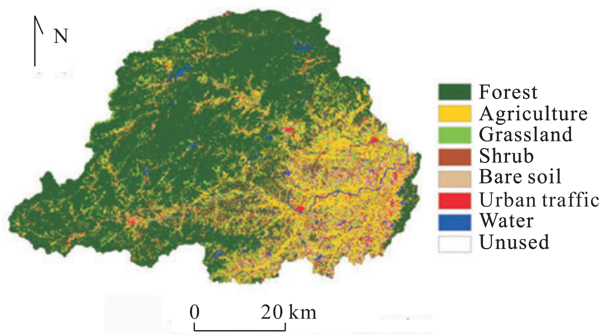

Figure 2. RS imagery-based land use classification of Liao watershed.

The watershed has experienced high deforestation rates from 1958 to 1960s. As a result, the vegetated mountains were transformed into bare land, which led to severe soil erosion (Zhang, 1990). A series of best management practices (BMPs), such as constructing terrace and strip cropping, and returning fields into forests have been applied since the 1980s in the watershed (Jiang and Kong, 2003), but the soil erosion rate is still high. The assessment of soil erosion and sediment yield is vital for soil conservation planning. Therefore, areas of higher erosion potential need to be identified before effective erosion control practices are developed and implemented (Mitra et al., 1998).

METHODS

The overall methodology involved the use of USLE in a GIS environment and the development of a spatial-varied SDR module. Individual raster layers were derived for each factor in USLE and processed in GIS. Sediment yield was computed using the proposed SDR module along with USLE. Taking into account both resolutions of source data and the area of the studied watershed, the 100 m grid size was considered to be the most reasonable compared with some other resolutions examined by the authors.

Soil Erosion Model

The USLE was developed to estimate long-term average annual soil erosion and originally applied for plane area at plot scale. Studies in mountainous areas at the watershed level have been also conducted, and the sound results verified its capability of modeling the complex landscapes (Lufafa et al., 2003; Mati et al., 2000). It is expressed as follows

$$A=R\times K\times L\times S\times C\times P \quad (1)$$

where A is annual soil erosion (t/ha/a); R is the rainfall erosivity factor (MJ·mm/ha/h); K is the soil erodibility factor (t·h/MJ/mm); L is the slope length factor; S is the slope steepness factor; C is the crop and management factor; and P is the conservation supporting practices factor.

Rainfall erosivity factor (*R*)

The R factor represents the rainfall and runoff's impact on soil, which is the product of storm rainfall energy (E) and the maximum 30-minute intensity (I30) (Brown and Foster, 1987). For areas that have no detailed climate data, R can be estimated using a modified Fournier index (F). Arnoldus (1977) proposed a modified form of the Fournier index in order to avoid drawbacks related to the monthly distribution of erosive rainfall during the year, and it was used to establish erosion risk areas in North Africa and the Middle East by FAO.

$$F=\sum_{i=1}^{12}\frac{r_i^2}{P} \quad (2)$$

where r_i is the precipitation in the month and P is the annual precipitation.

A relationship between R and F can be determined by regression analysis. Arnoldus (1977) computed the equation as R=0.264$F^{1.50}$, which was used to develop an iso-erodent map for Morocco. Similarly, the regression equations with R and F were obtained by Zhang and Fu (2003) for Jiangxi Province, China, as R=0.359 8$F^{1.946\ 2}$. Ahmet et al. (2007) suggested that the equation is R=0.121 5$F^{2.242\ 1}$ when estimating R for the Seyhan River basin in Turkey. These results show that the association between R and F varies widely among different climatic zones. Zhang's equation was used in this study because it was derived under climate conditions similar to the study area.

Soil erodibility factor (*K*)

The K factor measures soil susceptibility to rill and interrill erosion. It depends on the physical and chemical properties of soils, such as texture, aggregate stability, shear strength, infiltration capacity, organic matter content, etc. (Nisar et al., 2000). Liang and Shi (1999) determined K values for great soil groups in China using the soil erodibility factor monograph in conjunction with a soil map. The detailed soil properties they used were acquired from China's Second Soil Survey. As for this study, a K value map was obtained by assigning these values to the soil map of the watershed.

Topographic factor (*LS*)

The effect of slope length and gradient on the intensity of the erosion process is collectively known as the "topographic factor, *LS*" (Nisar et al., 2000). They are best determined by field measurement. However, fieldwork is both time consuming and labor extensive for the studied watershed. Therefore, a DEM-based procedure developed in USA (van Remortel et al., 2004; Hickey, 2000; Hickey et al., 1994) was employed to resolve the difficulties arising from the estimation of the *LS*-factor on a regional scale. The algorithms of this procedure use the raster grid cumulation and maximum downhill slope methods. In this way, each cell of the grid surface of the watershed was assigned an *LS* value.

Crop and management factor (*C*)

The C factor in the USLE represents the effect of cropping and management practices in agricultural management and the effect of ground, tree, and grass covers on reducing soil loss in nonagricultural situations (Wang et al., 2002). It measures the combined effect of all the interrelated cover and crop management variables (Folly et al., 1996). The *C* factor can be evaluated by allocating published *C* values to corresponding land cover classes (Lee, 2004). The remote sensing provides an opportunity to assess land cover at any place on the earth's surface. For the Liao watershed, a Landsat ETM+ image acquired on 14 September 2000 was geo-referenced to the Universal Transverse Mercator (UTM) projection. An unsupervised classification was performed, and the watershed was classified into forest, agriculture, grass, shrub, bare soil, urban and traffic, and unused (Fig. 2). The *C* map was obtained by assigning classified land cover classes with representative values from USLE guide tables (Morgan, 1995; Wischmeier and Smith, 1978).

Erosion control practice factor (*P*)

The erosion control practice factor is defined as the ratio of soil loss with a given surface condition to soil loss with up-and-down-hill plowing. It was thought as the most difficult factor to determine and was the least reliable factor of the USLE input factors (Renard et al., 1994). As for Liao watershed, the erosion control practice factor (*P*) was roughly determined from the land use classification map and the *P* factor table that is based on interpolation from Wischmeier and Smith (1978).

SDR Module

The USLE cannot be directly used to estimate the amount of sediment reaching downstream areas because some portion of the eroded soil may be deposited while traveling to the downstream point of interest (Lim et al., 2005). To account for these processes, the SDR is used to estimate the total sediment transported to the watershed outlet. The values of SDR for an area are affected by catchment physiography, sediment sources, transport system, texture of eroded material, land cover, etc. (Walling, 1988, 1983). Williams and Berndt (1974) found that the average channel slope is more significant than other parameters in estimating SDR, which is expressed as follows

$$\mathrm{SDR}=0.627\mathrm{SLP}^{0.403} \quad (3)$$

where the SLP (%) is slope of the main stream channel. This equation was considered to give a reasonable estimation of the SDR in cases where data are inadequate (Onyando et al., 2005).

In this article, a spatially distributed SDR module was developed based on equation (3). The module can compute the SDR for each cell in the flow path. To produce a spatially distributed SDR map, the flow path was generated from the DEM using ArcHydro Tools (Maidment, 2002). Then, the average slope value in % for each cell in the flow path was computed in a GIS to derive average channel slope values for the estimation of the SDR value for that cell using equation (3). Each cell in the flow path can be viewed as the outlet of its upstream catchment. Therefore, the SDR value of that cell measures the sediment delivery capacity of its upstream catchment. The sediment yield at each cell could be obtained by multiplying the SDR value of that cell with the computed soil erosion amount upstream from that cell. The distributed SDR map extends the SDR from watershed level to cell level; thus, it can be used for the identification of sediment source areas and the prediction of sediment yield at a point of interest. Therefore, it provides the guidance for the allocation of soil conservation practices.

RESULTS AND DISCUSSION

Factors in USLE

Seven meteorological stations spread in or around the watershed were identified, and monthly rainfall data over a time span from 1971 to 2000 were collected. The monthly average rainfall data and computed rainfall erosivity factor (*R*) are listed in Table 1. The *R* was found to range from 5 733.4 to 12 628.0 MJ·mm/ha/h, showing climatologically high erosion potential. The seasonal variability in precipitation amounts and the EI are very important to evaluate the seasonal risk of erosive storm events (Renschler et al., 1999). As can be seen in Table 1, most of the precipitation occurs in May, June, and July. This may suggest that most of the erosion occur within the rainy season and largely during some major storms. The discrete data were then interpolated into a continuous *R* value map (Fig. 3a) using the inverse distance weighted interpolation method.

The *K* factor value for each soil type was obtained from previous studies, which can be found in Table 2. The erodibility of soils varied from 0.015 8 to 0.030 4 t·h/MJ/mm. The most easily erodible soil is only distributed in the easternmost part of the watershed with very small coverage. The soil with the hardest erosion is in the middle and eastern parts of the study area and does not account for a large area. The rest of the watershed is occupied by soils with relatively moderate erodibility. The *K* factor map (Fig. 3b) was prepared by assigning the *K* value to each soil type in the soil map. We assume that all the soils in the study area have three erodibility values. Such an assumption neglects the subtle differences among different soil types and may introduce errors or lead to inaccuracy in the erosion estimation because the result greatly depends on the details of soil classifications.

The *LS* factor was calculated by using SRTM DEM with a resolution of 90 m. The result shows that the *LS* value ranges from 0 to 132.8. It can be seen from the *LS* map (Fig. 3c) that the low *LS* value is distributed along the valleys of the Liao River and its tributaries, especially in the east where the land is

Table 1 Monthly average of rainfall and annual rainfall-runoff erosivity for each meteorological station

Station	Rainfall (mm)												Erosivity (MJ·mm/ha/h)
	Jan.	Feb.	Mar.	Apr.	May	Jun.	Jul.	Aug.	Sept.	Oct.	Nov.	Dec.	
Xiushui	70.2	93.6	147.9	222.9	215.4	299.4	177.9	116.7	84.6	78.9	63.6	42.6	8 521
Lushan	75.9	99.6	157.5	224.1	258.0	315.9	249.9	289.2	149.1	115.5	85.5	48.0	12 628
Nanchang	74.1	100.8	175.5	223.8	243.9	306.6	144.0	129.0	68.7	59.7	56.7	41.4	9 284
Pingjiang	72.9	89.4	146.1	198.0	214.2	251.7	174.3	134.7	73.2	76.8	60.9	39.9	7 162
Ji'an	73.4	103.2	169.0	224.4	214.6	234.0	116.3	134.5	79.6	74.2	55.0	40.7	7 042
Jiujiang	51.8	95.0	137.0	183.6	193.1	213.7	141.0	131.8	95.5	96.5	64.8	40.3	5 733
Jiayu	58.5	73.2	124.5	166.3	188.3	244.8	163.0	123.6	75.1	95.7	64.4	36.8	6 017

Table 2 *K* values for major soils

Soil type	Red soil	Brown soil	Weakly developed red soil
K value (t·h/MJ/mm)	0.030 4	0.015 8	0.029 9

Table 3 *LS* value distribution

LS factor range	0–10	10–30	30–50	50–80	>80
Area (km^2)	2 479	936	104	10.9	0.4
Area percentage (%)	70.22	26.51	2.95	0.31	0.01

Table 4 Land cover classes and *C* values in the Liao watershed

Land cover type	Area (km^2)	Percentage (%)	*C* value
Forest	2 087.54	59.1	0.003
Agriculture	514.76	14.6	0.63
Shrub	343.07	9.7	0.014
Grass	213.88	6.1	0.05
Bare soil	139.49	4.0	1.0
Urban and traffic	117.17	3.3	0.003
Unused	63.31	1.8	1.0
Water	50.90	1.4	0.0

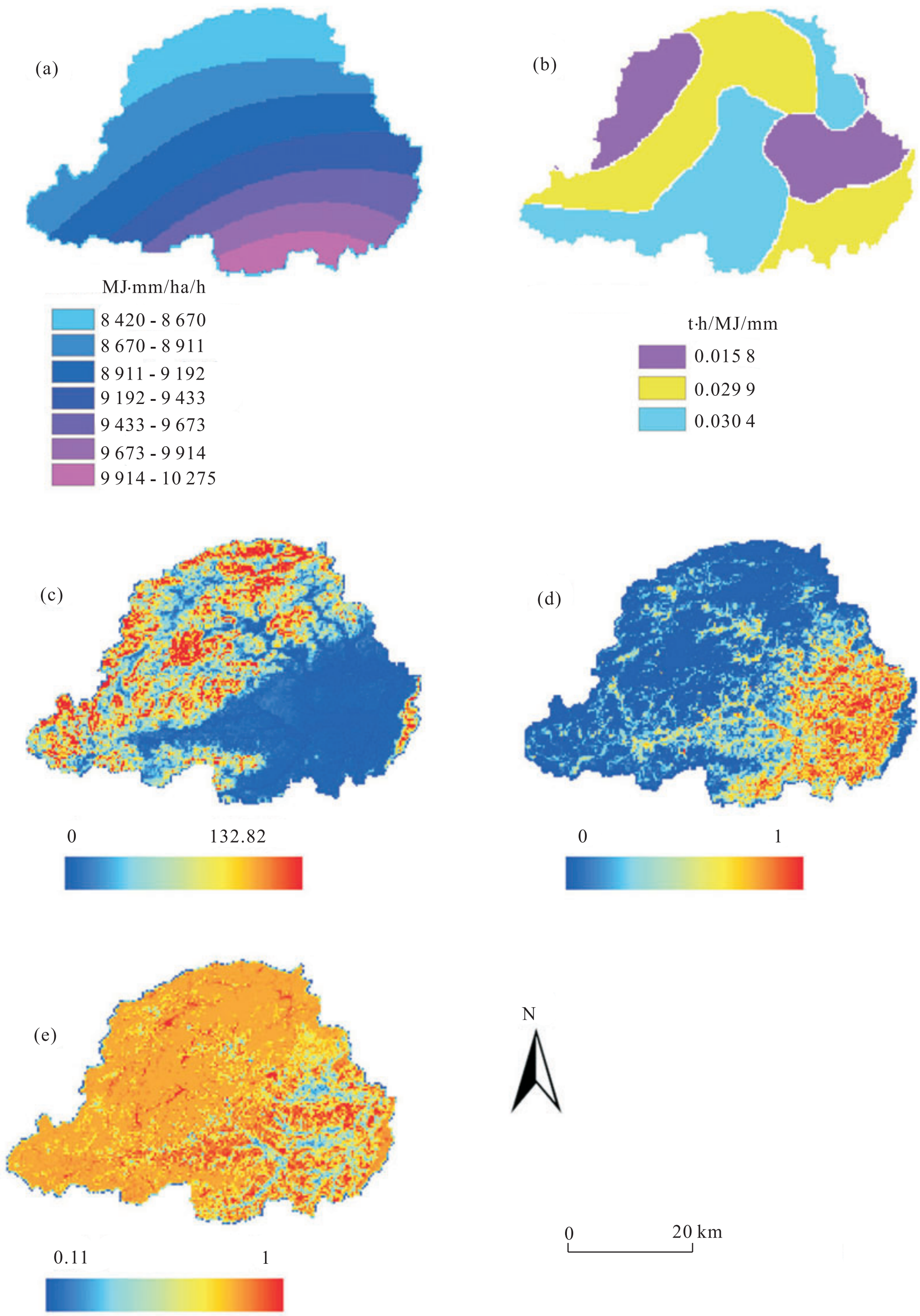

Figure 3. Spatial distribution of USLE input factors. (a) *R* factor map, (b) *K* factor map, (c) *LS* factor map; (d) *C* factor map; and (e) *P* factor map.

suitable for cultivation and habitation. The high *LS* value is found in the mountainous area with steep topography. Table 3 illustrates the distribution of *LS* values. According to the table, 70.22% of the area is under 10, which indicates that this portion of the region is not topographically prone to be eroded. *LS* values between 10 and 30 account for 26.51% of the watershed, and the *LS* between 30 and 50 covers 2.95% of the area. The rest with high *LS* value of more than 50 and very high value of more than 80 account for 0.31% and 0.01% of the area, respectively. The great variations of *LS* values can be ascribed to the complex mountainous landforms of the watershed, which is very typical in erosion-stricken areas of

South China. Although the *LS* value was not verified in the field, the testing results by van Remortel et al. (2004) showed that this method has produced *LS*-factor values that mimic those generated by the original AML as well as the RUSLE Handbook estimates.

The classified land cover map of the watershed is presented in Fig. 2. The map of *C* factor (Fig. 3d) was generated by reclassification of each land cover type using *C* values given in Table 4. From the table, a total of 74.9% of the watershed was covered by forest, shrub, and grass (59.1%, 9.7%, and 6.1%, respectively), while agriculture totally covered 14.6%. Bare soil, urban and traffic, unused, and water entirely enveloped 10.5% of the watershed (4.0%, 3.3%, 1.8%, and 1.4%). Therefore, *C* map of the watershed is mainly comprised of values of 0.03 and 0.63, respectively, for forest and agriculture. The higher *C* factor values indicate higher soil erosion potential as the *C* factor is a ratio of soil loss in a cover management sequence to soil loss from the bare soil unit plot (Nyakatawa et al., 2001).

It is generally revealed in Fig. 3d that most of mountainous areas in the watershed are well covered with vegetation except some places in the eastern and northeastern parts with severe deforestation, resulting in very high *C* values, which might lead to serious erosion. Southeast of the watershed is a big valley characterized by extensive agricultural development and is highly populated, which also shows potential for soil erosion. The method assumes that the same land covers have the same *C* factor values. In fact, the same land cover class may have different *C* values due to variations in vegetation density (Lu et al., 2004). Thus, Lu et al. (2004) suggested that the use of multitemporal remotely sensed data may be necessary to generate an average *C* factor map. In this study, constant cover management factor (*C*) values were used instead of time varying values because of the lack of a series of land cover maps for different years. Improved results can be expected if these enhancements are incorporated.

The *P* factor map (Fig. 3e) was prepared from the spatial analysis program in GIS based on Table 5, which shows the relationship between the *P* factor and slope levels for various land use types. The values of *P* factors of the Liao watershed were found to range from 0.11 to 1.0 with a mean value of 0.35.

Table 5 Erosion control practice factor (*P*)

Land use type	Slope (%)	*P* factor
Agriculture	0–5	0.11
	5–10	0.12
	10–20	0.14
	20–30	0.19
	30–50	0.25
	>50	0.33
Forest	0–200	0.8
Others	0–200	1.0

Erosion Intensity

The USLE input layers in raster format were resampled to a 100 m grid using a bilinear method. The soil erosion is estimated by the USLE as a product of *R*, *K*, *LS*, *C*, and *P*. The average soil erosion for the watershed was 18.2 t/ha/a with a standard deviation of 109.3 t/ha/a. The average rate far exceeds the 5 t/ha/a soil loss tolerance limit given for the study areas. The soil erosion and its spatial distribution can provide a basis for comprehensive management and sustainable land use at the watershed scale. According to the soil erosion classification criterion of China (Table 6), the soil erosion was grouped into six classes, which are presented in Fig. 4. About 39.5% of the watershed is under the tolerant erosion rate. 60.5% of the study area undergoes erosion to different extents, among which 6.6%, 2.7%, 4.0%, and 6.7% suffer from moderate, severe, very sever, and extremely severe erosion, respectively (Fig. 5).

Table 6 Soil erosion classes and ranges of soil erosion

Class	EC1 Very slight	EC2 Slight	EC3 Moderate	EC4 Severe	EC5 Very severe	EC6 Extremely severe
Range (t/ha/a)	0–5	5–25	25–50	50–80	80–150	>150
Soil depth (mm/a)	<0.37	0.37–1.9	1.9–3.7	3.7–5.9	5.9–11.1	>11.1

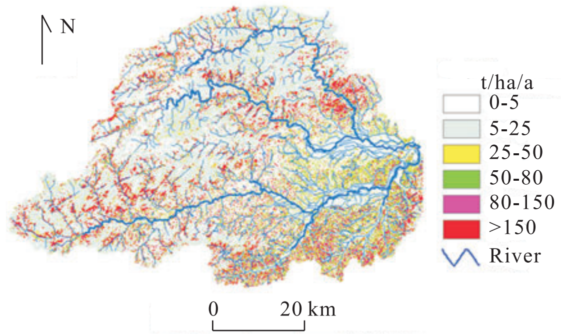

Figure 4. Erosion classification map of Liao watershed.

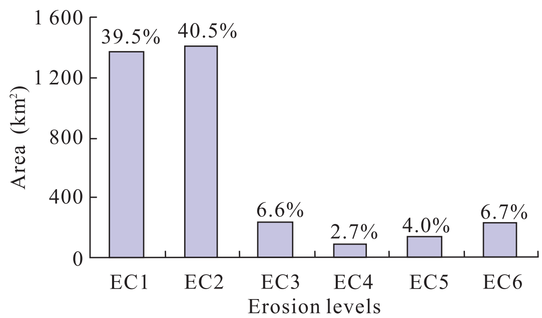

Figure 5. Diagraph of erosion classification.

These results reflect observations made in the field during a reconnaissance survey. The areas with extremely severe erosion, namely, more than 150 t/ha/a, were observed in the field to have experienced severe erosion as evidenced by many gullies and poor vegetation cover. Such areas have very steep slopes indicating the significance of percent slope in determining soil erosion. This conforms with the relationship that erosion increases proportionally with square of slope. It is clearly illustrated that the patterns in the erosion map (Fig. 4) are similar to those of the *LS* (Fig. 3c) and *C* value maps (Fig. 3d). Natalia (2005) also found that the *LS* and *C* measurements are highly correlated with those of erosion in terms of spatial patterns. This indicates that the soil erosion is very sensitive to the *LS* and *C* factors. Those findings imply that soil conservation measures should be aimed to decrease field slope, shorten flow length and provide better protection of the soil surface.

Sediment Yield

The SRTM DEM of Liao watershed was obtained. Then, the flow path was generated based on the flow accumulation matrix with a threshold of 500 by ArcHydro Tools (Maidment, 2002). This threshold was chosen because it can produce the best flow path compared with the blue line map. The slope-based SDR map of the flow path was created for the watershed (Fig. 6). The SDR values range from 0.04 to 0.57, which are closely related to the slope of the watershed. From the map, the SDR values in the northwest part of the watershed (upstream) are higher than those in the southeast part (downstream) because steeper topography occurs in the northwest region. Therefore, more eroded soil in the upstream areas will be transported into the channels and delivered out of the watershed. The SDR map was considered reasonable because it reflects that the ultimate nature of sediment delivery that erosion occurs in the steeper location will have more chances to be transported into the channels than to be deposited downslope.

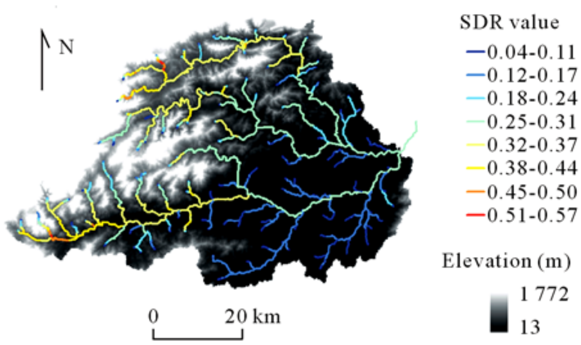

Figure 6. Slope-based SDR map at flow path draped over DEM.

The SDR value at the outlet of Liao watershed is estimated as 0.206. Chai (1996) reported that the SDR in this region is under 0.3, indicating that the values of SDR of this magnitude are expected in the Liao watershed. Given that the soil erosion amount for the entire watershed was calculated as 6.42 million t/a, the sediment yield was found to be 1.32 million t/a. E et al. (2004) reported that the measured sediment is 1.1 million t/a for this watershed. Thus, the estimated value is 20% higher than that of the measured yield. If the average deviation of the USLE model is less than 20%, the simulation is considered acceptable as asserted by Bingner et al. (1989). Therefore, the soil erosion estimation in this study is within the acceptable level of accuracy.

The overestimation may stem from the soil erosion model. It is well known that the USLE was not developed for this kind of environment. Many studies showed that USLE substantially overestimates soil erosion and sediment yield in such settings due to sediment deposition in irregular and long slopes (Hamlett et al., 1992; Johnson, 1988; Trimble and Lund, 1982). The precision of data used in this study is also problematic. Because the detailed data of climate, land cover, and soil are not available, the coarser data are used instead. The inaccuracy in the input data will lead to errors of the output. The data problems are very typical for large watersheds especially in developing countries where data are not readily available.

CONCLUSIONS

This study is an attempt to estimate soil erosion and sediment yield in the Liao watershed using USLE, RS, and GIS. It is clear from the results that, even if some uncertainties and inaccuracies are present, the USLE model can be efficiently applied at the watershed scale with the modest data requirements. The use of GIS enabled the determination of the magnitude and spatial distribution of the biophysical parameters. Consequently, thematic maps of the parameters and the estimated soil erosion were determined. The results show that 60.5% of the watershed undergoes erosion, and the average soil erosion is 18.2 t/ha/a. The areas that suffered from different soil erosion classes were identified based on the soil erosion classification criterion of China. With this information, management interventions can be precisely focused and priority should be given to areas with severe erosion.

The sediment yield from the Liao watershed was found in this study as 1.32 million t/a, which is 20% higher than that of the measured yield. The SDR value used to derive this figure was 0.206. This value was estimated using the proposed SDR module that was used to derive spatially distributed SDR values for the flow path. This module can be used for the identification of sediment source areas and prediction of sediment yield with available optimum data sets. The results suggest that a large quantity of eroded soil was delivered out of the watershed. The resultant sediments have already reduced the storage of Poyang Lake and endangered the ecosystem of the lake's wetlands. Therefore, it is suggested that this watershed needs immediate attention from a soil conservation point of view.

Although the results of this study are considered acceptable, due to the limitation of USLE, spatial heterogeneity in the watershed, and use of empirical data, there are still uncertainties in the calculated value. In further studies, more attention should be paid to the accuracy of USLE-factors and data precision.

ACKNOWLEDGMENTS

This work was supported by China Technological Supporting Program (No. 2007BAC23B05), the Special Research Fund for Prevention of Geological Disasters in Three Gorges Reservoir Area (No. SXKY3-6-1), the Natural Science Foundation of Hubei Province (No. 2009CDB104), and the Opening Foundation of State Key Laboratory for Information Engineering in Surveying, Mapping, and Remote Sensing, Wuhan University (No. (09)Key 01).

REFERENCES CITED

Ahmet, I., Fatih, T., Veli, U., 2007. Estimating Spatial Distribution of Soil Loss over Seyhan River Basin in Turkey. *Journal of Hydrology*, 336: 30–37

Arnoldus, H. M. J., 1977. Methodology Used to Determinate the Maximum Potential Average Soil Loss due to Sheet and Rill Erosion in Marocco: Assessing Soil Degradation. *FAO Soils Bull.*, 34: 8–9

Bahadur, K. C. K., 2009. Mapping Soil Erosion Susceptibility Using Remote Sensing and GIS: A Case of the Upper Name Wa Watershed, Nan Province, Thailand. *Environmental Geololy*, 57(3): 695–705

Bakoariniaina, L. N., Kusky, T., Raharimahefa, T., 2006. Disappearing Lake Alaotra: Monitoring Catastrophic Erosion, Waterway Silting, and Land Degradation Hazards in Madagascar Using Landsat Imagery. *Journal of African Earth Sciences*, 44(2): 241–252

Bartsch, K. P., van Miegroet, H., Boettinger, J., et al., 2002. Using Empirical Erosion Models and GIS to Determine Erosion Risk at Camp William, Utah. *J. Soil Water Conserv.*, 57(1): 29–37

Beskow, S., Mello, C. R., Norton, L. D., et al., 2009. Soil Erosion Prediction in the Grande River Basin, Brazil Using Distributed Modeling. *Catena*, 79(1): 49–59

Bhattarai, R., Dutta, D., 2007. Estimation of Soil Erosion and

Sediment Yield Using GIS at Catchment Scale. *Water Resources Management*, 21(10): 1635–1647

Bingner, R. L., Murphree, C. E., Mutchler, C. K., 1989. Comparison of Sediment Yield Models on Various Watershed in Mississippi. *Trans. ASAE*, 32(2): 529–534

Brown, L. C., Foster, G. R., 1987. Storm Erosivity Using Idealized Intensity Distributions. *Trans. ASAE*, 30: 379–386

Cerri, C. E. P., Dematte, J. A. M., Ballester, M. V. R., et al., 2001. GIS Erosion Risk Assessment of the Piracicaba River Basin, Southeastern Brazil. *Mapping Sci. Remote Sensing*, 38: 157–171

Chai, Z. X., 1996. On Land Erosion in South China. *Mountain Research*, 14(4): 215–220 (in Chinese with English Abstract)

E, J. P., Liu, N., Deng, J., 2004. Sediment Bulletin for China Rivers. Chinese Ministry of Water Resources, Beijing, China (in Chinese with English Abstract)

Fistikoglu, O., Harmancioglu, N. B., 2002. Integration of GIS with USLE in Assessment of Soil Erosion. *Water Resources Management*, 16(6): 447–467

Flügel, W. A., Märker, M., Moretti, S., et al., 2003. Integrating Geographical Information Systems, Remote Sensing, Ground Truthing and Modelling Approaches for Regional Erosion Classification of Semi-arid Catchments in South Africa. *Hydrological Processes*, 17(5): 929–942

Folly, A., Bronsveld, M. C., Clavaux, M., 1996. A Knowledge-Based Approach for *C* Factor Mapping in Spain Using Landsat TM and GIS. *International Journal of Remote Sensing*, 17(12): 2401–2415

Hamlett, J. M., Miller, D. A., Day, R. L., et al., 1992. Statewide GIS-Based Ranking of Watersheds for Agricultural Pollution Prevention. *Journal of Soil and Water Conservation*, 47(5): 399–404

Hickey, R., 2000. Slope Angle and Slope Length Solutions for GIS. *Cartography*, 29(1): 1–8

Hickey, R., Smith, A., Jankowski, P., 1994. Slope Length Calculations from a DEM within ARC/INFO GRID. *Comput. Environ. Urban Syst.*, 18(5): 365–380

Jian, M. K., Kothyari, U. C., 2000. Estimation of Soil Erosion and Sediment Yield Using GIS. *Hydrol. Sci. J.*, 45(5): 771–786

Jain, S. K., Kumar, S., Varghese, J., 2001. Estimation of Soil Erosion for a Himalayan Watershed Using a GIS Technique. *Water Resources Management*, 15(1): 41–54

Jiang, W. S., Kong, F. B., 2003. Countermeasures for Water and Soil Erosion and Forest Ecosystem Management in Poyang Lake Watersheds. *Forest Resources Management*, 6: 36–40 (in Chinese with English Abstract)

Johnson, R., 1988. Putting Soil Movement into Perspective. *Journal of Production Agriculture*, 1(1): 5–12

Lee, S., 2004. Soil Erosion Assessment and Its Verification Using the Universal Soil Loss Equation and Geographic Information System: A Case Study at Boun, Korea. *Environmental Geology*, 45(4): 457–465

Liang, Y., Shi, X. Z., 1999. Soil Erodiable *K* in East Hillyfields of the Southern Yangtze River. *Research of Soil and Water Conservation*, 6(2): 47–52 (in Chinese with English Abstract)

Lim, K. J., Sagong, M., Engel, B. A., et al., 2005. GIS-Based Sediment Assessment Tool. *Catena*, 64(1): 61–80

Lin, C. Y., Lin, W. T., Chou, W. C., 2002. Soil Erosion Prediction and Sediment Yield Estimation: The Taiwan Experience. *Soil and Tillage Research*, 68(2): 143–152

Lu, D., Li, G., Valladares, G. S., et al., 2004. Mapping Soil Erosion Risk in Rondonia, Brazilian Amazonia: Using RULSE, Remote Sensing and GIS. *Land Degrad. Develop.*, 15(5): 499–512

Lufafa, A., Tenywa, M. M., Iasbirye, M., et al., 2003. Prediction of Soil Erosion in a Lake Victoria Basin Catchment Using a GIS-Based Universal Soil Loss Model. *Agricultural Systems*, 76(3): 883–894

Maidment, D. R., 2002. Arc Hydro: GIS for Water Resources. ESRI Press, Redlands, CA

Mati, B. M., Morgan, R. P. C., Gichuki, F. N., et al., 2000. Assessment of Erosion Hazard with the USLE and GIS: A Case Study of the Upper Ewaso Ng'iro North Basin of Kenya. *International Journal of Applied Earth Observation and Geoinformation*, 2(2): 78–86

Meyer, L. D., Bauer, A., Heil, R. D., 1985. Experimental Approaches for Quantifying the Effect of Soil Erosion on Productivity. In: Follett, R. F., Stewart, B. A., Ballew, I. Y., eds., Soil Erosion and Crop Productivity. American Society of Agronomy, Crop Science Society of America and Soil Science Society of America Publishers, Madison, WI, USA. 213–234

Mitra, B., Scott, H. D., Dixon, J. C., et al., 1998. Applications of Fuzzy Logic to the Prediction of Soil Erosion in a Large Watershed. *Geoderma*, 86(3–4): 183–209

Morgan, R. P. C., 1995. Soil Erosion and Conservation. John Wiley & Sons, Essex, England

Morgan, R. P. C., Quinton, J. N., Smith, R. E., et al., 1998. The European Soil Erosion Model (EUROSEM): A Dynamic

Approach for Predicting Sediment Transport from Fields and Small Catchments. *Earth Surface Processes and Landforms*, 23(6): 527–544

Natalia, H., 2005. Spatial Modeling of Soil Erosion Potential in a Tropical Watershed of the Colombian Andes. *Catena*, 63: 85–108

Nearing, M. A., Lane, L. J., Lopes, V. L., 1994. Modeling Soil Erosion. In: Lal, R., ed., Soil Erosion: Research Methods. St. Lucie Press, Delray Beach, FL. 127–135

Nisar, T. R., Ahamed, K., Rao, G., et al., 2000. Fuzzy Class Membership Approach to Soil Erosion Modelling. *Agricultural Systems*, 63: 97–110

Nyakatawa, E. Z., Reddy, K. C., Lemunyon, J. L., 2001. Predicting Soil Erosion in Conservation Tillage Cotton Production Systems Using the Revised Universal Soil Loss Equation (RUSLE). *Soil & Tillage Research*, 57(4): 213–224

Onyando, J. O., Kisoyan, P., Chemelil, M. C., 2005. Estimation of Potential Soil Erosion for River Perkerra Catchment in Kenya. *Water Resources Management*, 19(2): 133–143

Oyedele, J. D., 1996. Effects of Erosion on the Productivity of Selected Southwestern Nigerian Soils: [Dissertaion]. Department of Soil Science, Obafemi Awolowo University, Ile-Ife, Nigeria

Ozcan, A. U., Erpul, G., Basaran, M., et al., 2008. Use of USLE/GIS Technology Integrated with Geostatistics to Assess Soil Erosion Risk in Different Land Uses of Indagi Mountain Pass—Cankiri, Turkey. *Environmental Geology*, 53(8): 1731–1741

Pan, J. J., Zhang, T. L., Zhao, Q. G., 2005. Dynamics of Soil Erosion in Xingguo County, China, Determined Using Remote Sensing and GIS. *Pedosphere*, 15(3): 356–362

Pandey, A., Chowdary, V. M., Mal, B. C., 2007. Identification of Critical Erosion Prone Areas in the Small Agricultural Watershed Using USLE, GIS and Remote Sensing. *Water Resources Management*, 21(4): 729–746

Renard, K. G., Foster, G. R., Weesies, G. A., et al., 1997. Predicting Soil Erosion by Water: A Guide to Conservation Planning with the Revised Universal Soil Loss Equation (RUSLE). Agriculture Handbook No. 703, USDA Agricultural Research Services, Washington, DC

Renard, K. G., Laflen, J. M., Foster, G. R., et al., 1994. The Revised Universal Soil Loss Equation. In: Lal, R., ed., Soil Erosion Research Methods. St. Lucie Press, Delray Beach, FL. 105–124

Renschler, C. S., Mannaerts, C., Diekkrüeger, B., 1999. Evaluating Spatial and Temporal Variability in Soil Erosion Risk—Rainfall Erosivity and Soil Loss Ratios in Andalusia, Spain. *Catena*, 34(3–4): 209–225

Rodda, H. J. E., Demuth, S., Shankar, U., 1999. The Application of a GIS Based Decision Support System to Predict Nitrate Leaching to Groundwater in Southern Germany. *Hydrol. Sci. J.*, 44(2): 221–236

Shi, Z. H., Cai, C. F., Ding, S. W., et al., 2004. Soil Conservation Planning at the Small Watershed Level Using RUSLE with GIS: A Case Study in the Three Gorge Area of China. *Catena*, 55(1): 33–48

Trimble, S. W., Lund, S. W., 1982. Soil Conservation and the Reduction of Erosion and Sedimentation in the Coon Creek Basin, Wisconsin. *U.S. Geological Survey Professional Paper*, 1234: 35

van Remortel, R. D., Maichle, R. W., Hickey, R. J., 2004. Computing the LS Factor for the Revised Universal Soil Loss Equation through Array-Based Slope Processing of Digital Elevation Data Using a C++ Executable. *Computers & Geosciences*, 30(9–10): 1043–1053

Walling, D. E., 1983. The Sediment Delivery Problem. *J. Hydrol.*, 65(1–3): 209–237

Walling, D. E., 1988. Erosion and Sediment Yield Research—Some Recent Perspectives. *J. Hydrol.*, 100(1–4): 113–141

Wang, G. X., Gertner, G., Fang, S. F., et al., 2003. Mapping Multiple Variables for Predicting Soil Loss by Geostatistical Methods with TM Images and a Slope Map. *Photogramm. Eng. Remote Sens.*, 69(8): 889–898

Wang, G., Wente, S., Gertner, G. Z., et al., 2002. Improvement in Mapping Vegetation Cover Factor for the Universal Soil Loss Equation by Geostatistical Methods with Landsat Thematic Mapper Images. *International Journal of Remote Sensing*, 23(18): 3649–3667

Wang, G. Q., Hapuarachchi, H., Ishidaira, H., 2009. Estimation of Soil Erosion and Sediment Yield during Individual Rainstorms at Catchment Scale. *Water Resources Management*, 23(8): 1447–1465

Williams, J. R., Berndt, H. D., 1974. Sediment Yield Computed with Universal Equation. *J. Hydraul. Div.*, 100(HY11): 1719–1720

Wischmeier, W. H., Smith, D. D., 1978. Predicting Rainfall Erosion Losses: A Guide to Conservation Planning, Agricultural Handbook 537. U.S. Department of Agriculture, Science and Education Administration, Washington, DC

Young, R. A., Onstad, C. A., Bosch, D. D., et al., 1987. An Agricultural Non-point Source Pollution Model, a Watershed

Analysis Toll. U.S. Department of Agricultural Research Services, Conservation Research Report 35

Zhang, R. F., 1990. Impaction of Soil and Water Loss to the Ecological Environment and Economy Construction of the Poyang Lake Watershed. *Acta Conservationis Soli et Aquae Sinica*, 4(3): 80–86 (in Chinese with English Abstract)

Zhang, W. B., Fu, J. S., 2003. Rainfall Erosivity Estimation under Different Rainfall Amount. *Resources Science*, 25(1): 35–41 (in Chinese with English Abstract)

Zhou, W. F., Wu, B. F., 2008. Assessment of Soil Erosion and Sediment Delivery Ratio Using Remote Sensing and GIS: A Case Study of Upstream Chaobaihe River Catchment, North China. *International Journal of Sediment Research*, 23(2): 167–173